

Structured Attention Graphs for Understanding Deep Image Classifications

Vivswan Shitole, Fuxin Li, Minsuk Kahng, Prasad Tadepalli, Alan Fern

School of Electrical Engineering and Computer Science, Oregon State University
{shitolev, lif, kahngm, tadepall, afern}@oregonstate.edu

Abstract

Attention maps are popular tools of explaining the decisions of convolutional networks for image classification. Typically, for each image of interest, a single attention map is produced, which assigns weights to pixels based on their importance to the classification. We argue that a single attention map provides an incomplete understanding since there are often many other maps that explain a classification equally well. In this paper, we introduce *structured attention graphs* (SAGs), which compactly represent sets of attention maps for an image by capturing how different combinations of image regions impact the confidence of a classifier. We propose an approach to compute SAGs and a visualization for SAGs so that deeper insight can be gained into a classifier's decisions. We conduct a user study comparing the use of SAGs to traditional attention maps for answering counterfactual questions about image classifications. Our results show that the users answer comparative counterfactual questions better when presented SAGs compared to attention map baselines.

1 Introduction

One of the long-standing open problems in deep learning for image classification is to help human users understand the decisions of a neural network (Hinton, McClelland, and Rumelhart 1986). This is important since deep neural networks (DNNs) function in a significantly different manner from humans. This is evident, for example, in their lack of robustness to outliers, which can result in many errors when the testing set is distributed differently from the training set (Goodfellow, Shlens, and Szegedy 2014; Hendrycks and Gimpel 2016). If DNNs are to be employed in crucial decision-making scenarios, such as perception for vehicles, robots, and medicine, their unexpected errors could have devastating consequences. Ideally, a visualization tool would help users to discover the source of those errors, which can lead to subsequent efforts to repair them.

A popular line of research towards this goal has been to display attention maps, sometimes called saliency maps or heatmaps. Most approaches assign weights to image regions based on the importance of that region to the classification decision, which is then visualized to the user. This approach

implicitly assumes that a *single attention map* with region-specific weights is sufficient for the human to construct a reasonable mental model of the classification decision for the particular image. Rather, deep networks are able to confidently classify an image based on different combinations of image regions. This is similar in nature to a human's ability to recognize objects under many different occlusion conditions. A single attention map, at best, is only able to indicate a single set of important regions. However, it is often the case that the importance of a region depends on what other regions are also visible.

Fig. 1 shows an example image where a single attention map gives limited insight into the behavior of a DNN's classifications. The two standard singleton attention maps shown in Fig. 1b-c provide some insight into the image regions the DNN finds important. However, it is unclear, which ones could stand on their own, which ones could be removed, or which combinations are critical for high confidence. In contrast, Fig. 1d-f show three localized attention maps of different regions, each of which, if presented as the input to the DNN, results in a very confident prediction on the correct category. These three maps provide insight into the DNN classification behavior that cannot be inferred from the standard maps. However, there are potentially many such localized maps, which are related to one another. A key challenge is to somehow reveal these types of insights to a human without overwhelming them.

The goal of this work is to construct a succinct visual representation that enables the users to acquire a reasonably expressive mental model on the behavior of a deep network, at least with respect to a given image. To this end, we propose *Structured Attention Graphs* (SAGs), which are directed acyclic graphs over attention maps of different image regions. The maps are connected based on containment relationships between the regions, and each map is accompanied with the confidence scores of the classification based on the map (see Fig. 2 for an example).

With this new visualization, users can view a diverse set of part combinations that could make the DNN classify an image as a certain class. In addition, by observing how the confidence changes across related maps it is possible to see the relative importance of sub-regions or patches in the context of other regions. For example, observing that the removal of a particular patch leading to a huge drop in the confi-

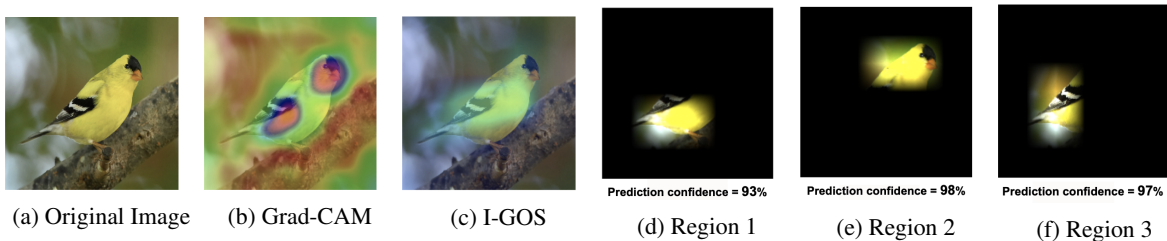


Figure 1: An image (a) predicted as Goldfinch with two attention maps (b) and (c) obtained from different approaches as explanation for the classifier’s (VGG-Net) prediction. Each of these attention maps creates a narrow understanding of the classifier. In (d), (e) and (f), we present three diverse regions of the image that are not deemed important by the singleton attention maps (b) and (c), and yet can be predicted by the same classifier as high confidence for the predicted class.

dence suggests that this patch is important in that context. This provides a more complete picture of the DNN classification landscape and thus helps the user form a better mental model. Computationally, we produce the SAGs via a heuristic search algorithm guided by confidence and diversity.

We can view our visualization as representing a Monotone Disjunctive Normal Form (MDNF) Boolean expression, where propositional symbols correspond to primitive image regions we call ‘patches’. Each MDNF expression is a disjunction of conjunctions, where any one of the conjunctions (e.g., one of the regions in Fig. 1) is sufficient for a high confident classification. We call them minimal sufficient conditions (MSCs). Each conjunction is true only when all the patches that correspond to its symbols are present in the image. The expressions are monotone, i.e., without negation, because with a few exceptions the confidence in the classification monotonically increases when more patches are included in the image. The SAG (shown in Fig. 2) is a directed acyclic graph whose roots represent the MSCs, nodes represent the different sub-terms of the MSCs, and edges represent the direct containment relationships between them.

With a better understanding of the network, we would hope the users to be able to answer more difficult predictive questions about the decision-making of the networks. For example, a simple counterfactual question might ask how a black-box model classifies an image when different parts of the image are blurred. In our user study, we go one level deeper and ask the subjects questions about which of two blurred versions of the image will be classified more positively. A user with an ideal mental model will be able to answer most of the counterfactual questions consistently with the black-box classifier.

In summary, our contributions include:

- We introduce Structured Attention Graphs (SAGs) as a novel representation to visualize image classification by deep neural networks.
- We propose a heuristic search algorithm and pruning rules to efficiently compute the SAG visualization in high-resolution images.
- We present a user study for evaluating SAGs, and its results indicate that our method outperforms two state-of-the-art attention map visualization approaches.

2 Related Work

Our work is related to and inspired by a number of prior works on explaining convolutional neural networks. As suggested earlier, much recent work on interpretability is based on different ways to generate attention maps of importance of different regions to the classification decisions. These include *gradient-based methods* that compute the gradient of the outputs of different units with respect to pixel inputs (Zeiler and Fergus 2014; Simonyan, Vedaldi, and Zisserman 2014; Springenberg et al. 2015; Shrikumar et al. 2016; Sundararajan, Taly, and Yan 2017; Bach et al. 2015; Shrikumar et al. 2016; Zhang et al. 2016; Selvaraju et al. 2017), *perturbation-based methods*, which perturb parts of the input to see which ones are most important to preserve the final decision (Dabkowski and Gal 2017; Fong and Vedaldi 2017), and *concept-based methods*, which analyze the alignment between individual hidden neurons and a set of semantic concepts (Bau et al. 2017; Kim et al. 2018; Zhou et al. 2018). Importantly, they all generate a single attention map for the image and do not attempt to evaluate the insights gained by the human users from these visualizations through counterfactual queries.

Another popular approach is LIME (Ribeiro, Singh, and Guestrin 2016), which constructs simplified interpretable local classifiers consistent with the black-box classifier in the neighborhood of a single example. However, the local classifier learns a single linear function, which is sufficient to correctly classify the image but does not guarantee consistency with the classifier on its sub-images. A more recent approach called Anchors (Ribeiro, Singh, and Guestrin 2018) learns multiple if-then-rules that represent sufficient conditions for classification of the image. The if-then-rules can be thought of as different terms of an MDNF expression represented by the root nodes in our SAG. SAG differs from it in additionally presenting the entire graph besides the root nodes, thus enabling users to understand the effects of removing different patches to the classification. The ablation study of Section 4.3 throws some light on the differences between the two approaches.

Some prior work identifies explanations in terms of minimal necessary features (Dhurandhar et al. 2018) and minimal sufficient features (Dabkowski and Gal 2017). Other work generates counterfactuals that are coherent with the underlying data distribution and provides feasible paths to

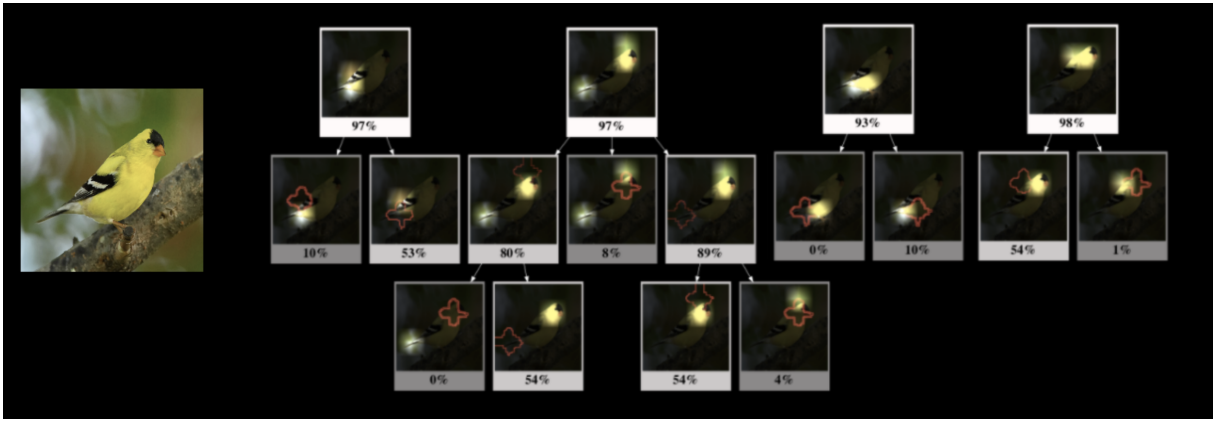


Figure 2: Example of a SAG. It is structured as a directed acyclic graph with each root node representing a minimal region of the image sufficient to achieve a high confidence for the classifier’s prediction. Each child node is obtained by deleting a patch (denoted by red contour) from the parent, causing a drop in the classifier’s confidence. A big drop in confidence implies the removed patch was of high importance to the classifier. More examples of SAGs are provided in the appendix.

the target counterfactual class based on density weighted metrics (Poyiadzi et al. 2020). In contrast, our work yields explanations in terms of minimal sufficient features and answers the counterfactual question – “how will the classification score change if some of these features are absent?”

Network distillation methods that compile a neural network into a boolean circuit (Choi et al. 2017) or a decision tree (Liu, Wang, and Matwin 2018) often yield uninterpretable structures due to their size or complexity. Our work balances the information gain from explanations with the interpretability of explanations by providing a small set of diverse explanations.

Traditional attention map approaches that yield a single map as explanation have been found to be brittle and unreliable (Kindermans et al. 2017; Ghorbani, Abid, and Zou 2019). This motivates the existence of multiple attention maps that together constitute a comprehensive and reliable explanation.

3 Constructing Structured Attention Graphs

In this section, we introduce Structured Attention Graphs (SAGs) which provide a human-interpretable explanation of a black-box classifier f . The SAGs enable human users to answer counterfactual queries about the classification of the instances represented in them. We assume that f maps $X \times C \rightarrow [0, 1]$, where X is an instance space and C is a set of classes and represents the confidence of classification. If $x \in X$ is an instance, we use $f_c(x)$ to denote $f(x, c)$, where $c \in C$ is a class. When X is a set of images, each instance $x \in X$ is seen as a set of pixels and is divided into r^2 non-overlapping primitive regions p_i called ‘patches,’ i.e., $x = \cup_{i=1}^{r^2} p_i$, where $p_i \cap p_j = \emptyset$ if $i \neq j$.

3.1 Structured Attention Graphs

For any instance $x \in X$, we let $f^*(x) = \operatorname{argmax}_c f(x, c)$ and call $f^*(x)$ the target class of x . We associate the part of the image in each patch with a propositional symbol or

a *literal*. A *conjunction* N of a set of literals is the image region that corresponds to their union. The *score* of a conjunction is the output of the classifier f applied to it $f(N, c)$. We determine this by running the classifier on a perturbed image where the pixels in $x \setminus N$ are either set to zeros or to a highly blurred version of the original image. The latter method is widely used in attention map visualization methods to remove information without creating additional spurious boundaries that can distort the classifier predictions (Fong and Vedaldi 2017; Petsiuk, Das, and Saenko 2018; Qi, Khorram, and Fuxin 2020).

A Structured Attention Graph (SAG) is a directed acyclic graph whose nodes correspond to conjunctions of image patches and edges represent *sub-conjunction* relationships defined as removal of a single patch from the conjunction. The goal of the representation and visualization of SAGs is to improve the human user’s *understanding* of the classifier f . We measure understanding indirectly with *predictive power*, which can be defined as the capability of predicting $f(N, c)$ given a new conjunction $N \subset x$ that has not been shown. Given that humans do not excel on giving numerical prediction values, we focus on answering *comparative queries*, which predict the TRUE/FALSE value of the query: $\mathbb{I}(f(N_1, c) > f(N_2, c))$, with \mathbb{I} being the indicator function.

We require each root conjunction N_i in the SAG to be a minimal region that has a high prediction confidence ($f(N_i, c) > P_h f_c(x)$), where we set $P_h = 90\%$ in our experiments. This means that if we feed only the minimal region represented in a root conjunction to the classifier, the classifier will yield a score greater than 90% for the class it predicted with the original (unblurred) image x as input. Typically, the score of a root conjunction N_i is higher than all its subconjunctions $n_j \subset N_i$. The size of the drop in the score may correspond to the importance of the removed patch $N_i \setminus n_j$. Under the reasonable assumption that the function f is monotonic with the set of pixels covered by the conjunction, the explanation problem generalizes learning Monotone DNF (MDNF) boolean expressions from

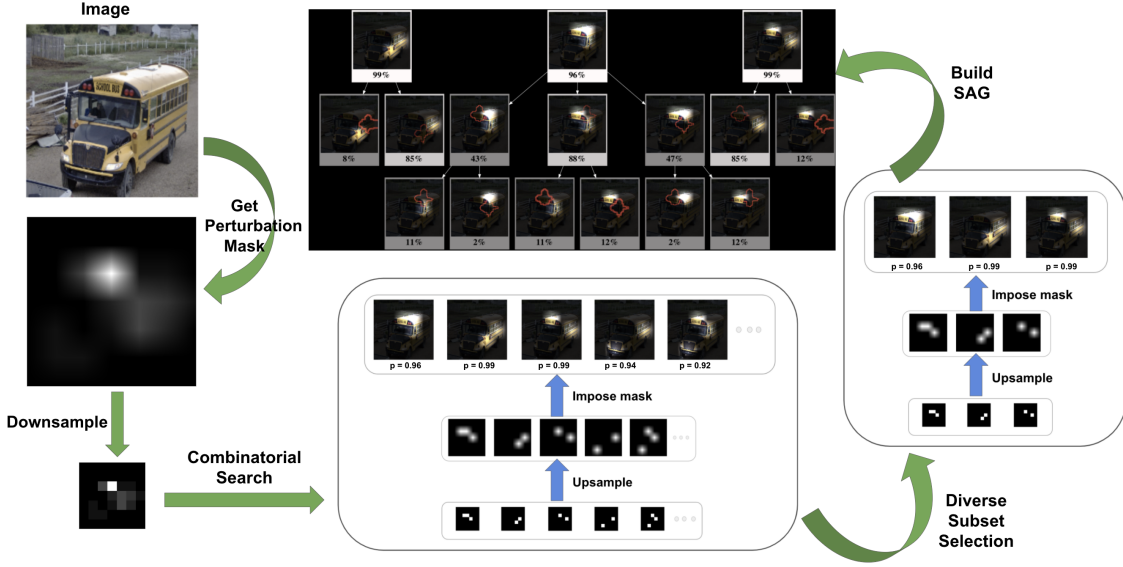


Figure 3: Illustration of the steps for generating a SAG from a given image

membership (yes/no) queries, where each disjunction corresponds to a root node of the SAG. Information-theoretic lower bounds imply that the general class of MDNF expressions is not learnable with polynomial number of membership queries although some special cases are learnable (Abasi, Bshouty, and Mazzawi 2014). In this work we employ a combinatorial search approach guided by a greedy heuristic pruning method to produce small-sized models. Our approach is summarized in Fig. 3.

3.2 Search for Minimal Sufficient Conjunctions

The objective of combinatorial search is to find minimal sufficient conjunctions of k patches N_k which score higher than a threshold, where no proper subsets exceed the threshold, i.e., find all N_k such that:

$$f_c(N_k) \geq P_h f_c(x), \max_{n_j \subset N_k} f_c(n_j) < P_h f_c(x) \quad (1)$$

for some high probability threshold P_h .

But this combinatorial search is too expensive to be feasible if we treat each image pixel as a patch. Hence we divide the image into a coarser set of non-overlapping patches. One could utilize a superpixel tessellation of an image to form the set of coarser patches. We adopt a simpler approach: we downsample the image into a small resolution $r \times r$ (e.g. 7×7). Each pixel in the downsampled image corresponds to a coarser patch in the original image. We then use a mask obtained from an attention map algorithm to further prune the set of patches. Given a mask M which gives nonnegative attention values on each pixel of an image, we first perform average pooling on M w.r.t. each patch p_j . This gives us an attention value $M(p_j)$ for each patch, hence constituting a coarser attention map. Then we select the top m patches with the highest $M(p_j)$ as our literals and perform a combinatorial search on them to find minimal subsets satisfying eq. (1). Besides, we prune the search tree at a certain depth,

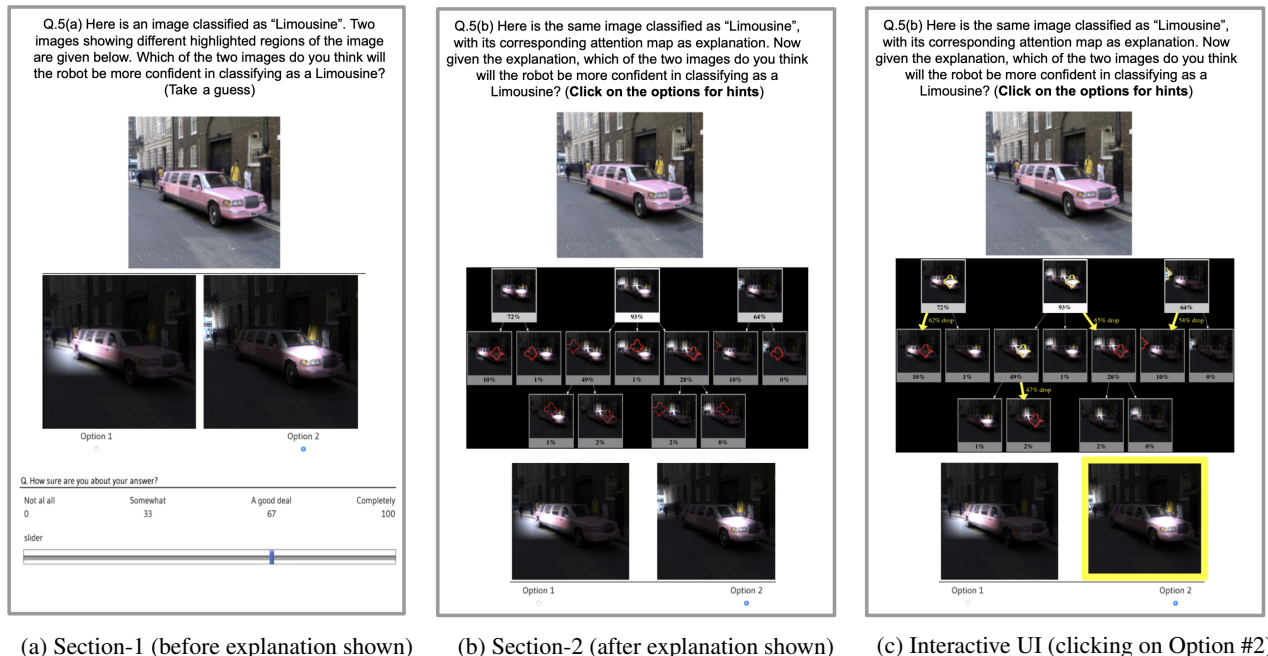
meaning that we would only allow root conjunctions with a maximal k literals in the solution. Hence the combinatorial search is reduced to the order of $\binom{m}{k}$, which is practically feasible. We chose $r = 7, m = 20$ and $k = 3$ as hyperparameters. Finally, we utilize bilateral upsampling to upsample the search results back to the original image dimensions.

3.3 Selecting a Diverse subset of Minimal Sufficient Conjunctions

Combinatorial search provides us a set of candidate minimal sufficient conjunctions (MSCs) as the solution: $\tilde{N}_{\text{candidates}} = \{\tilde{N}_1, \dots, \tilde{N}_t\}$, for some $t > 1$. We observe that the obtained set $\tilde{N}_{\text{candidates}}$ has a large number of similar conjunctions that share a number of literals. To minimize the cognitive burden on the user and efficiently communicate relevant information with a small number of conjunctions, we heuristically prune the above set to select a small diverse subset. Note that we prefer a diverse subset (based on dispersion metrics) over a representative subset (based on coverage metrics). This choice was based on the observation that even a redundant subset of candidates $\tilde{N}_{\text{redundant}} \subset \tilde{N}_{\text{candidates}}$ can achieve high coverage when the exhaustive set $\tilde{N}_{\text{candidates}}$ has high redundancy. But $\tilde{N}_{\text{redundant}}$ has lower information compared to a diverse subset of candidates $\tilde{N}_{\text{diverse}} \subset \tilde{N}_{\text{candidates}}$ obtained by optimizing a dispersion metric.

More concretely, we want to find an information-rich diverse solution set $\tilde{N}_{\text{diverse}} \subset \tilde{N}_{\text{candidates}}$ of a desired size c such that $|\tilde{N}_i \cap \tilde{N}_j|$ is minimized for all $\tilde{N}_i, \tilde{N}_j \in \tilde{N}_{\text{diverse}}$ where $i \neq j$. We note that $\tilde{N}_{\text{diverse}}$ can be obtained by solving the following subset selection problem:

$$\begin{aligned} \tilde{N}_{\text{diverse}} &= \underset{X \subseteq \tilde{N}_{\text{candidates}}, |X|=c}{\operatorname{argmin}} \psi(X), \\ \text{where } \psi(X) &= \max_{\tilde{N}_i, \tilde{N}_j \neq i \in X} |\tilde{N}_i \cap \tilde{N}_j| \end{aligned}$$



(a) Section-1 (before explanation shown)

(b) Section-2 (after explanation shown)

(c) Interactive UI (clicking on Option #2)

Figure 4: A question from our user study. The options users need to select from are different from any of the attention maps in the SAG shown to the users.

For any subset X of the candidate set, $\psi(X)$ is the cardinality of the largest pairwise intersection over all member sets of X . $\tilde{N}_{\text{diverse}}$ is the subset with minimum value for $\psi(X)$ among all the subsets X of a fixed cardinality c . Minimizing $\psi(X)$ is equivalent to maximizing a dispersion function, for which a greedy algorithm obtains a solution upto a provable approximation factor (Dasgupta, Kumar, and Ravi 2013). The algorithm initializes $\tilde{N}_{\text{diverse}}$ to the empty set, and at each step adds a new set $y \in \tilde{N}_{\text{candidates}}$ to it which minimizes $\max_{z \in \tilde{N}_{\text{diverse}}} |y \cap z|$. The constant c is set to 3 in order to show a sufficiently diverse and yet not overwhelming number of candidates in the SAG.

3.4 Patch Deletion to Build the SAG

After we have obtained the diverse set of candidates $\tilde{N}_{\text{diverse}}$, it is straightforward to build the SAG. Each element of $\tilde{N}_{\text{diverse}}$ forms a root node for the SAG. Child nodes are recursively built by deleting one patch at a time from a parent node (equivalent to obtaining leave-one-out subsets of a parent set). We calculate the confidence of each node by a forward pass of the image represented by the node through the deep network. Since nodes with low probability represent less useful conjuncts of patches, we do not expand nodes with probability less than a threshold P_l as a measure to avoid clutter in the SAG. P_l is set to 40% as a hyperparameter.

All the SAGs presented in the paper explain the predictions of VGG-Net (Simonyan and Zisserman 2014) as the classifier. Each SAG was generated within 30 seconds of wallclock time using a single Nvidia Tesla V100 GPU. The source code is provided in the appendix and will be made

publicly available upon publishing.

4 Evaluation via User Study

We conducted a user study to evaluate the effectiveness of our proposed SAG visualization. User studies have been a popular method to evaluate explanations. Grad-CAM (Selvaraju et al. 2017) conducted a user study to evaluate faithfulness and user trust on their attention maps. LIME (Ribeiro, Singh, and Guestrin 2016) asked participants to predict generalizability of their method by showing their explanations to the participants. This section describes the design of our study and its results.

4.1 Study Procedure

We designed our user study based on *counterfactual* questions since we believe these questions require a deeper understanding and a correct mental model of the classification mechanisms of the network to answer. Our questions require users to answer comparative queries as defined in Sec. 3.1, but on two new conjunctions as options that have not been shown in the SAG presented to them. Users need to predict which of the two options would receive a higher confidence score for the class predicted by the DNN for the original image. Fig. 4 shows an example of a question used in our study. The images constituting the questions were a random sample from a subset of ImageNet comprising of 10 classes. Along with the graph visualization, SAG provides users with an interactive interface (as shown in Fig. 4(c)) in which they can click on an option to highlight the corresponding nodes in the graph that have overlapping patches with the selected option. We compare our visualization with two state-of-the-art

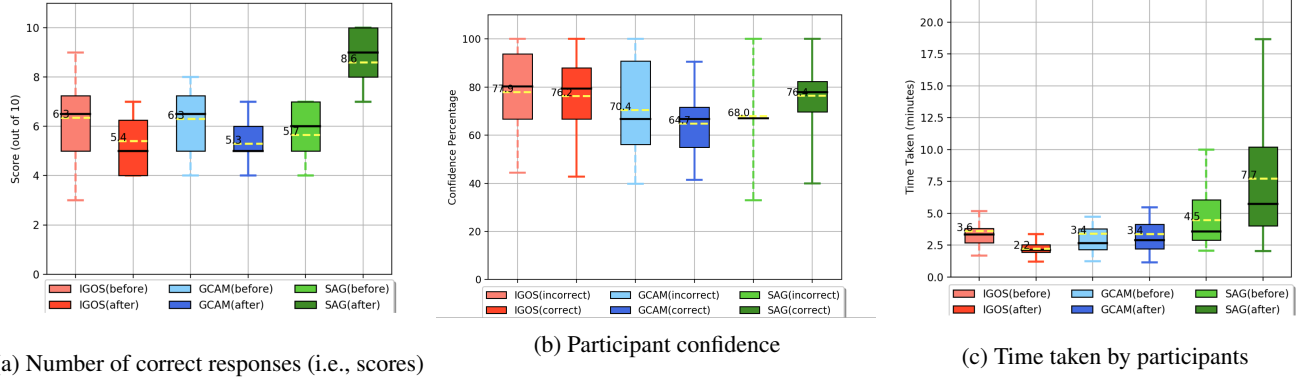


Figure 5: User study results comparing SAG to I-GOS and Grad-CAM. Dashed yellow lines in the box plots denote mean values.

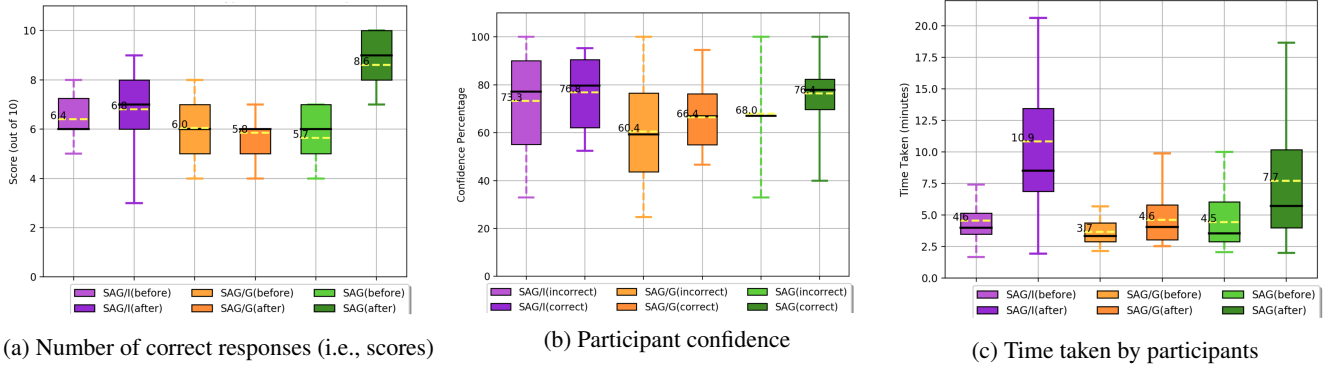


Figure 6: Ablation study results comparing SAG to SAG/I and SAG/G.

attention map approaches I-GOS (Qi, Khorram, and Fuxin 2020) and Grad-CAM (Selvaraju et al. 2017).

We recruited 60 participants comprising of graduate and undergraduate students in engineering students at our university (37 males, 23 females, age: 18-30 years). Participants were randomly divided into three groups with each group evaluating one of the three attention map approaches (i.e., between-subjects study). Each participant was first shown a tutorial informing them about the basics of image classification and attention maps as explanations for image classification. Then the participant was directed to the task that involved answering 10 questions with each question composed of two sections. In the first section, each participant is shown a reference image with its classification but no explanation. They are also shown two options which are two different perturbed versions of the reference image with different regions of the image blurred out. Participants are asked to select one of the options that they think would be more likely to be classified to the class predicted by the DNN for the original image. In the second section, the participants are shown the same reference image with the same options, but are also provided with an attention map or SAG as explanation for the classification decision. Participants are asked the same question to choose one of the two options, but this

time under the premise of the given visual explanation. The participants are required to provide a confidence rating notifying how sure they are about their response.

The metrics obtained from the user study include the number of correct responses among the 10 questions (i.e., score) for each participant, the confidence score for each of their response (i.e., 100 being completely confident; 0 being not at all), and the time taken to answer each response.

4.2 Results

Fig. 5 shows the results comparing the metrics across the three conditions. As we can see from Fig. 5(a), participants got more answers correct when they are provided with SAG explanations (mean=8.6, stddev=1.698) than when they are provided with I-GOS (mean=5.4, stddev=1.188) or Grad-CAM (mean=5.3, stddev=1.031) explanations. The differences between SAG and each of the two other methods are statistically significant (p -value<0.0001 in unpaired t-tests).

Fig. 5(b) shows the participants' levels of confidence for correct and incorrect answers across all three conditions after being provided with the explanations. The plots show that their confidence levels are almost the same for both correct and incorrect responses in case of I-GOS and Grad-CAM. However, for the case of SAG, participants have lower confi-

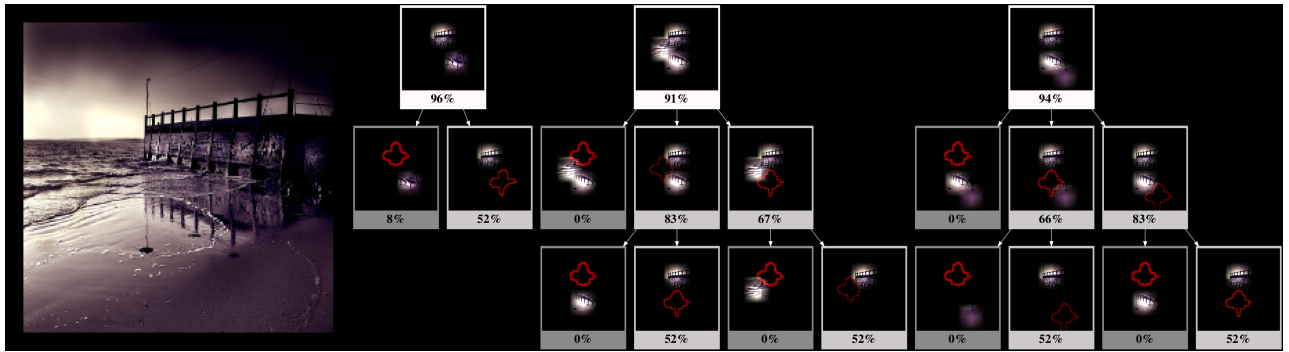


Figure 7: SAG explanation for the wrong classification of this image as “shopping cart”. Correct class is “seashore”.

dence for incorrect responses and higher confidence for correct responses. Interestingly, the variance in confidence for incorrect answers is very low for the participants working with SAG explanations. Increased confidence for correct responses and reduced confidence for incorrect responses implies that SAG explanations allow users to “know what they know” and when to trust their mental models. Indifference in confidence for correctness, as in the case of I-GOS and Grad-CAM, may imply that users lack a realistic assessment of the correctness of their mental models.

Fig. 5(c) shows that SAG explanations require more effort for participants to interpret explanations. This is expected because SAGs convey more information compared to other attention maps. However, we believe that the benefits of gaining the right mental models and “appropriate trust” justify the longer time users need to digest the explanations.

4.3 Ablation Study

The two major components of SAG are the graph-based attention map visualization and the interactive interface. As an ablation study, we include two ablated versions of SAGs in the user study: (1) SAG/I, which is a SAG without the interactive interface, comprising only of the graph visualization and (2) SAG/G, which is a SAG without the graph visualization, comprising only of the root nodes (root conjuncts) and the interactive interface. These root conjuncts are similar in spirit to the if-then rules of Anchors (Ribeiro, Singh, and Guestrin 2018) and serve as an additional baseline.

To evaluate how participants would work with SAG/I and SAG/G, we additionally recruited 40 new participants (30 males, 10 females, age: 18-30 years) from the same recruitment effort as for earlier experiments and split them into two groups, with each group evaluating an ablated version of SAGs via the aforementioned study procedure. The results of the ablation study are shown in Fig. 6. The participants received significantly lower scores when the UI interaction (SAG/I) or the graph structure (SAG/G) are removed (as in Fig. 6a). This implies that both the interactive interface and the graph structure are critical components of SAGs. The correlations of high confidence with correctness and low confidence with incorrectness are maintained across the ablated versions (as in Fig. 6b). Participants spent a longer time to interpret a SAG without the interactive interface, while interpreting just the root nodes took a shorter time (as in

Fig. 6c). The exhaustive data for all the 100 participants involved in the study is provided in the appendix.

4.4 Using SAGs for Debugging

SAGs can be particularly useful to gain insights about the predictions of a neural network and facilitate debugging in case of wrong predictions. For example, Fig. 7 shows that the image with ground truth class as “seashore” is (wrongly) classified as a “shopping cart” by VGG-Net because the coast fence looks like a shopping cart. Interestingly, the classifier uses the reflection of the fence as further evidence for the class “shopping cart”: with both the fence and the reflection the confidence is more than 83% but with only the fence it was 52%. The patch corresponding to the reflection is not deemed enough on its own for a classification of shopping cart (evident from the drop in probabilities shown in SAG). We provide many such examples of SAGs that yield insights into VGG-Net in the appendix.

5 Conclusions and Future Work

We presented a new representation and visualization to explain the behavior of black-box classifiers for image classification. The key idea is to recognize that robust decision making has more than one correct explanation and that an ideal visualization would make them explicit along with the contributions of different parts to the confidence of the decision. We also introduced a new way to evaluate the visualizations by testing the mental models of their human users on counterfactual queries. Results show that our approach lends itself to more robust mental models than the traditional attention maps which typically focus on a single explanation and fail to support nuanced inferences by their users.

There exist many interesting future research opportunities. One weakness of our approach is it takes more time for people to read SAGs than the existing methods. This could be mitigated via interfaces with more advanced interactive features that allow users to construct and explore SAGs based on their needs. This can be very useful for experts to interactively steer and probe the system to gain useful insights. Another direction is to generalize our approach to multiple images and apply our methodology to other modalities such as language and videos.

References

- Abasi, H.; Bshouty, N. H.; and Mazzawi, H. 2014. On Exact Learning Monotone DNF from Membership Queries 111–124.
- Bach, S.; Binder, A.; Montavon, G.; Klauschen, F.; Müller, K.; and Samek, W. 2015. On pixel-wise explanations for non-linear classifier decisions by layer-wise relevance propagation. *PLoS One* 10. ISSN 1932-6203. doi:10.1371/journal.pone.0130140.
- Bau, D.; Zhou, B.; Khosla, A.; Oliva, A.; and Torralba, A. 2017. Network Dissection: Quantifying Interpretability of Deep Visual Representations. In *Computer Vision and Pattern Recognition*.
- Choi, A.; Shi, W.; Shih, A.; and Darwiche, A. 2017. Compiling neural networks into tractable Boolean circuits. *intelligence*.
- Dabkowski, P.; and Gal, Y. 2017. Real Time Image Saliency for Black Box Classifiers. In *NIPS*.
- Dasgupta, A.; Kumar, R.; and Ravi, S. 2013. Summarization through submodularity and dispersion. In *Proceedings of the 51st Annual Meeting of the Association for Computational Linguistics (Volume 1: Long Papers)*, 1014–1022.
- Dhurandhar, A.; Chen, P.-Y.; Luss, R.; Tu, C.-C.; Ting, P.; Shanmugam, K.; and Das, P. 2018. Explanations based on the missing: Towards contrastive explanations with pertinent negatives. In *Advances in neural information processing systems*, 592–603.
- Fong, R. C.; and Vedaldi, A. 2017. Interpretable Explanations of Black Boxes by Meaningful Perturbation. In *2017 IEEE International Conference on Computer Vision (ICCV)*, 3449–3457.
- Ghorbani, A.; Abid, A.; and Zou, J. 2019. Interpretation of neural networks is fragile. In *Proceedings of the AAAI Conference on Artificial Intelligence*, volume 33, 3681–3688.
- Goodfellow, I. J.; Shlens, J.; and Szegedy, C. 2014. Explaining and harnessing adversarial examples. *arXiv preprint arXiv:1412.6572*.
- Hendrycks, D.; and Gimpel, K. 2016. A baseline for detecting misclassified and out-of-distribution examples in neural networks. *arXiv preprint arXiv:1610.02136*.
- Hinton, G. E.; McClelland, J. L.; and Rumelhart, D. E. 1986. Distributed representations. In Rumeihart, D. E.; McClelland, J. L.; and the PDP Research Group, eds., *Parallel distributed processing: Explorations in the microstructure of cognition: Vol. 1. Foundations*, 77–109. Cambridge, MA: MIT Press.
- Kim, B.; Wattenberg, M.; Gilmer, J.; Cai, C.; Wexler, J.; Viegas, F.; et al. 2018. Interpretability beyond feature attribution: Quantitative testing with concept activation vectors (tcav). In *International conference on machine learning*, 2668–2677. PMLR.
- Kindermans, P.-J.; Hooker, S.; Adebayo, J.; Alber, M.; Schütt, K. T.; Dähne, S.; Erhan, D.; and Kim, B. 2017. The (un) reliability of saliency methods. *arXiv preprint arXiv:1711.00867*.
- Liu, X.; Wang, X.; and Matwin, S. 2018. Improving the interpretability of deep neural networks with knowledge distillation. In *2018 IEEE International Conference on Data Mining Workshops (ICDMW)*, 905–912. IEEE.
- Petsiuk, V.; Das, A.; and Saenko, K. 2018. RISE: Randomized Input Sampling for Explanation of Black-box Models. In *Proceedings of the British Machine Vision Conference (BMVC)*.
- Poyiadzi, R.; Sokol, K.; Santos-Rodriguez, R.; De Bie, T.; and Flach, P. 2020. FACE: Feasible and actionable counterfactual explanations. In *Proceedings of the AAAI/ACM Conference on AI, Ethics, and Society*, 344–350.
- Qi, Z.; Khorram, S.; and Fuxin, L. 2020. Visualizing Deep Networks by Optimizing with Integrated Gradients. In *Proceedings of the AAAI Conference on Artificial Intelligence*.
- Ribeiro, M. T.; Singh, S.; and Guestrin, C. 2016. Why should i trust you?: Explaining the predictions of any classifier. In *Proceedings of the 22nd ACM SIGKDD international conference on knowledge discovery and data mining*, 1135–1144. ACM.
- Ribeiro, M. T.; Singh, S.; and Guestrin, C. 2018. Anchors: High-Precision Model-Agnostic Explanations. In McIlraith, S. A.; and Weinberger, K. Q., eds., *Proceedings of the Thirty-Second AAAI Conference on Artificial Intelligence*, 1527–1535. AAAI Press.
- Selvaraju, R. R.; Cogswell, M.; Das, A.; Vedantam, R.; Parikh, D.; and Batra, D. 2017. Grad-CAM: Visual Explanations from Deep Networks via Gradient-Based Localization. In *2017 IEEE International Conference on Computer Vision (ICCV)*, 618–626.
- Shrikumar, A.; Greenside, P.; Shcherbina, A.; and Kundaje, A. 2016. Not Just a Black Box: Learning Important Features Through Propagating Activation Differences. *CoRR* abs/1605.01713. URL <http://arxiv.org/abs/1605.01713>.
- Simonyan, K.; Vedaldi, A.; and Zisserman, A. 2014. Deep Inside Convolutional Networks: Visualising Image Classification Models and Saliency Maps. *ICLR Workshop*.
- Simonyan, K.; and Zisserman, A. 2014. Very deep convolutional networks for large-scale image recognition. *arXiv preprint arXiv:1409.1556*.
- Springenberg, J.; Dosovitskiy, A.; Brox, T.; and Riedmiller, M. 2015. Striving for Simplicity: The All Convolutional Net. In *ICLR Workshop*. URL <http://lmb.informatik.uni-freiburg.de/Publications/2015/DB15a>.
- Sundararajan, M.; Taly, A.; and Yan, Q. 2017. Axiomatic Attribution for Deep Networks. In Precup, D.; and Teh, Y. W., eds., *Proceedings of the 34th International Conference on Machine Learning*, 3319–3328. PMLR.
- Zeiler, M. D.; and Fergus, R. 2014. Visualizing and Understanding Convolutional Networks. In Fleet, D.; Pajdla, T.; Schiele, B.; and Tuytelaars, T., eds., *Computer Vision – ECCV 2014*, 818–833. Cham: Springer International Publishing.

Zhang, J.; Lin, Z.; Brandt, J.; Shen, X.; and Sclaroff, S. 2016. Top-down neural attention by excitation backprop. In *European Conference on Computer Vision*, 543–559. Springer.

Zhou, B.; Sun, Y.; Bau, D.; and Torralba, A. 2018. Interpretable Basis Decomposition for Visual Explanation. In *Proceedings of the European Conference on Computer Vision (ECCV)*.

6 Appendix A - User study data

Here we provide the scores of all the 100 users that participated in our user study. We see that the scores are fairly random when participants are not provided with any explanation. Moreover, participants spending more time on the questions do not necessarily achieve higher scores.

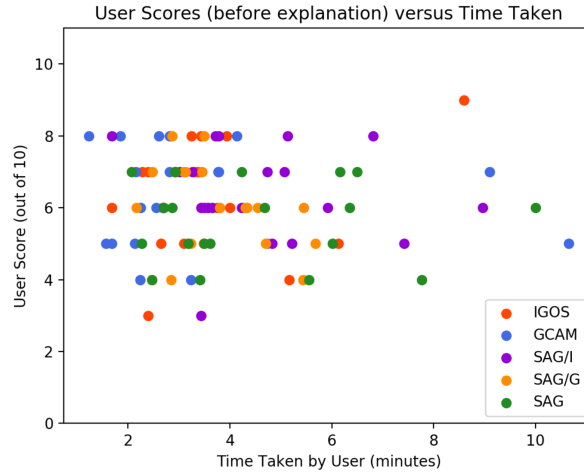


Figure 8: Performance versus Time scatter plot of all users before they are shown the explanations.

After providing the explanations, we see that high scores (8 and above) are exclusively obtained by participants working with SAG and its ablations. As discussed earlier, participants working with SAG and SAG/I tend to have a higher response time than participants working with other explanations.

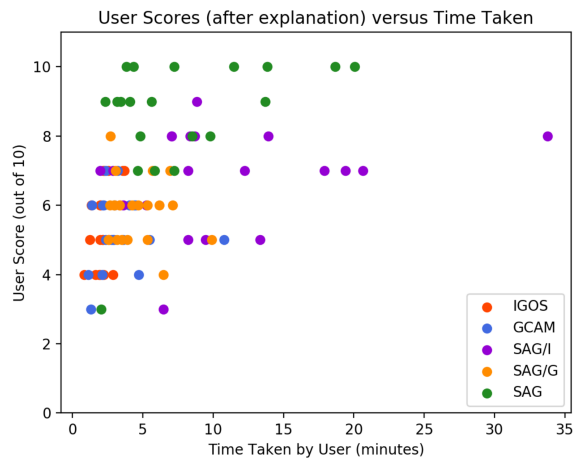


Figure 9: Performance versus Time scatter plot of all users after they are shown the explanations.

7 Appendix B - More examples of SAGs

Here we provide more examples of SAGs for various images with their predicted (true) classes. In order to emphasize the advantage of our approach over traditional attention maps, we also provide the corresponding Grad-CAM and I-GOS saliency maps.

7.1 Class: *Goldjay*



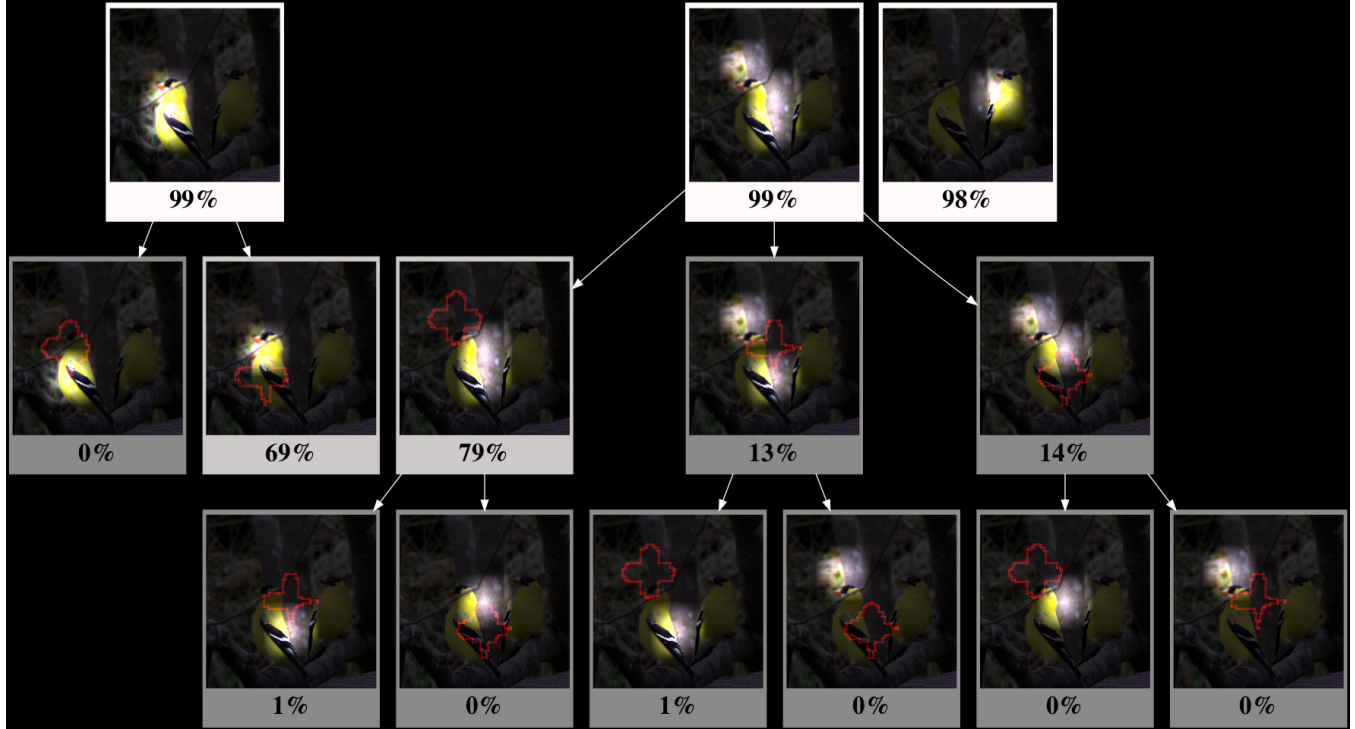
(a) Original Image



(b) Grad-CAM



(c) I-GOS



(d) SAG

7.2 Class: Schoolbus



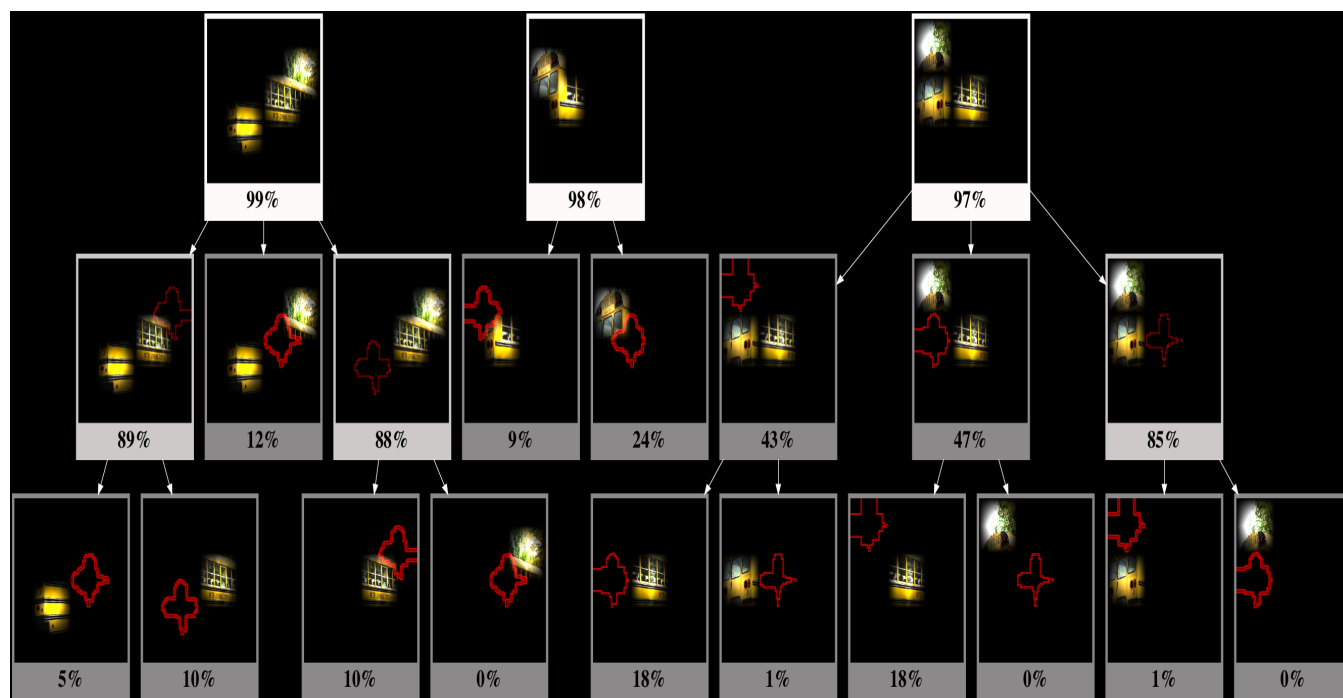
(a) Original Image



(b) Grad-CAM



(c) I-GOS

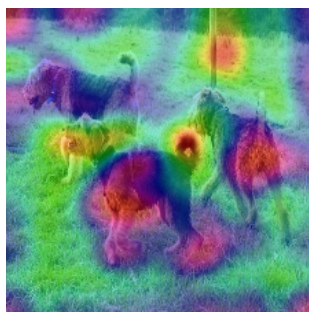


(d) SAG

7.3 Class: Airedale Terrier



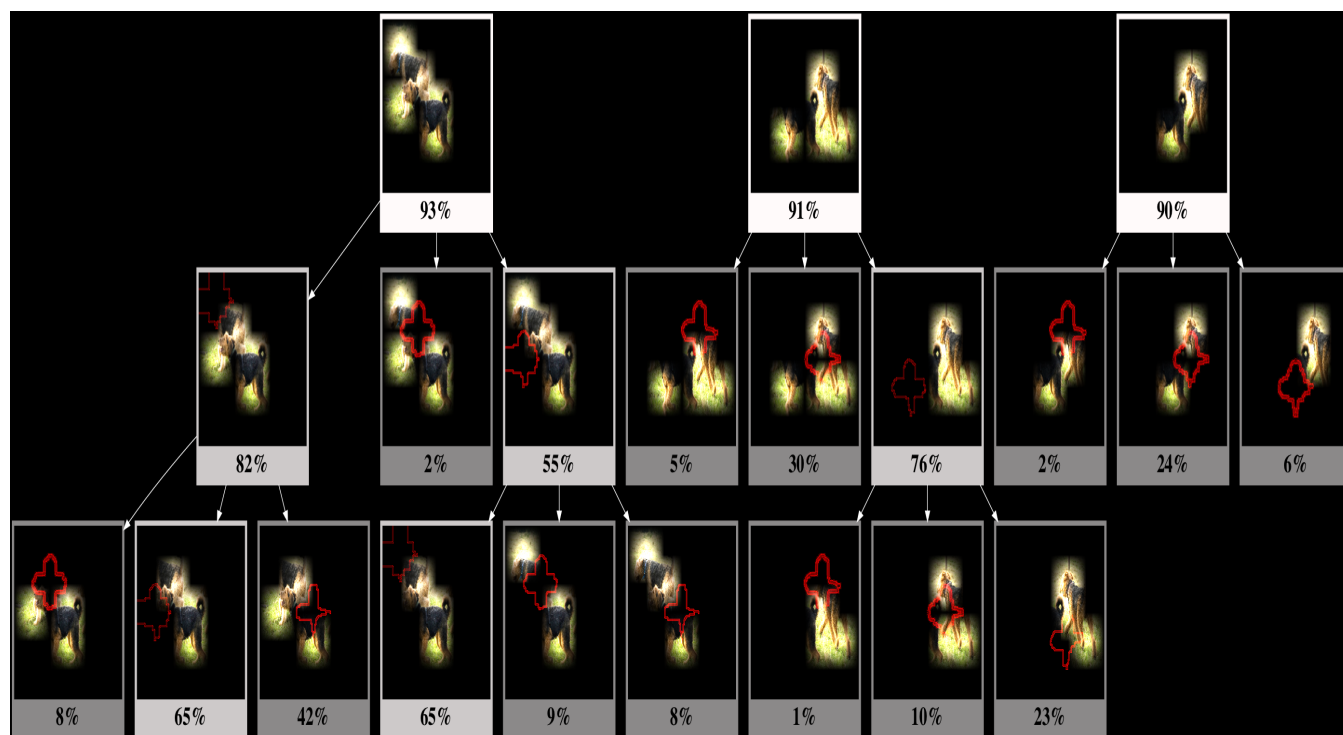
(a) Original Image



(b) Grad-CAM

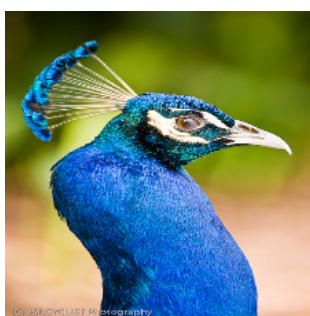


(c) I-GOS

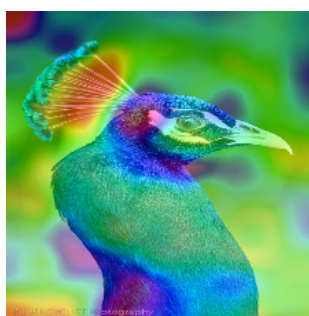


(d) SAG

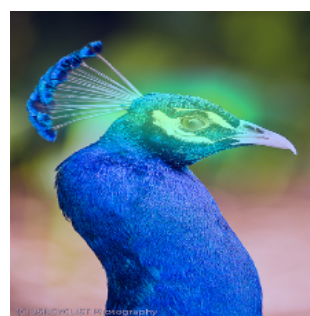
7.4 Class: *Peacock*



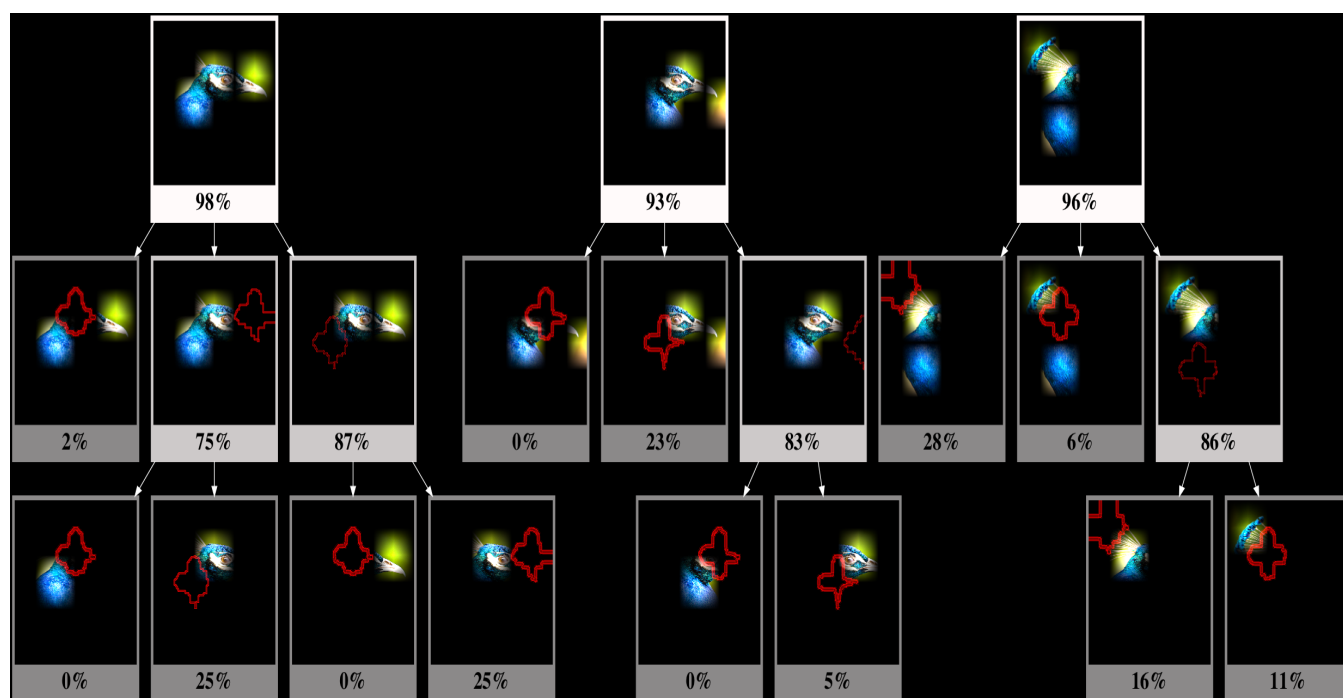
(a) Original Image



(b) Grad-CAM



(c) I-GOS



(d) SAG

7.5 Class: RV



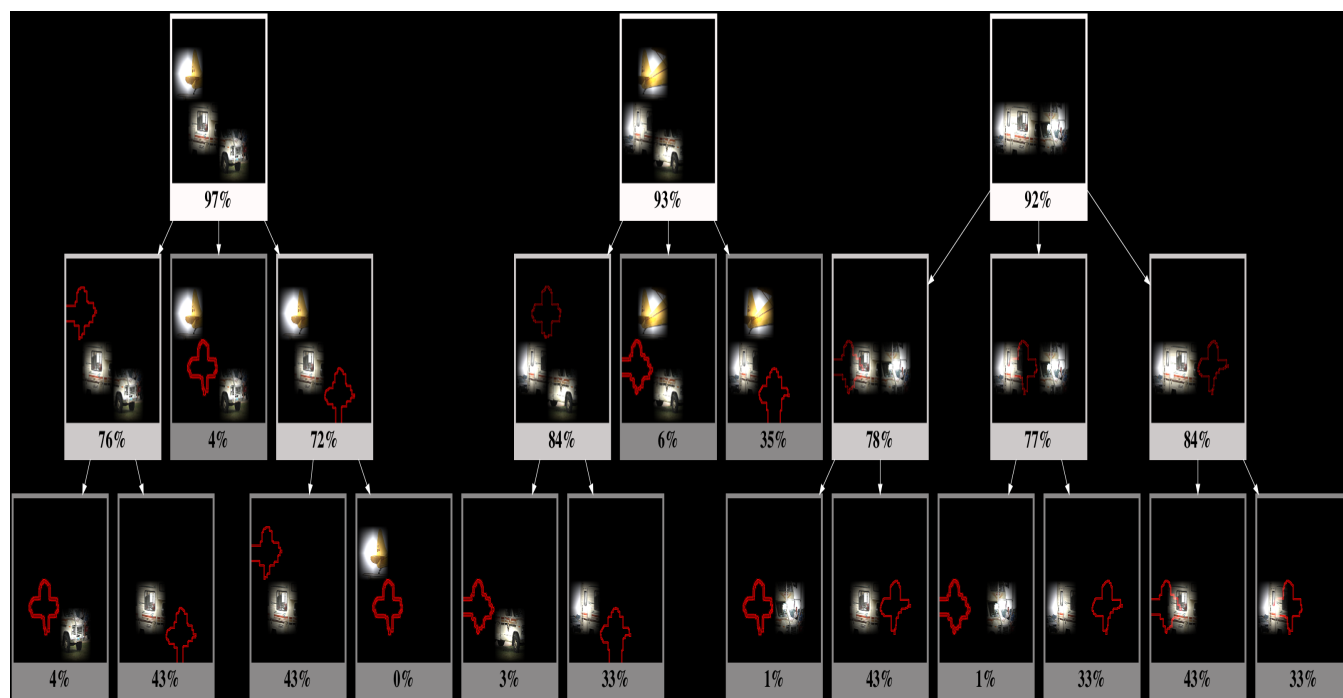
(a) Original Image



(b) Grad-CAM

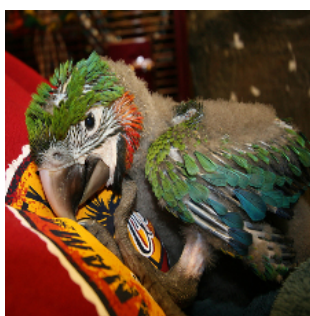


(c) I-GOS



(d) SAG

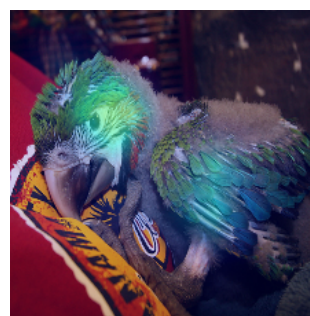
7.6 Class: *Macaw*



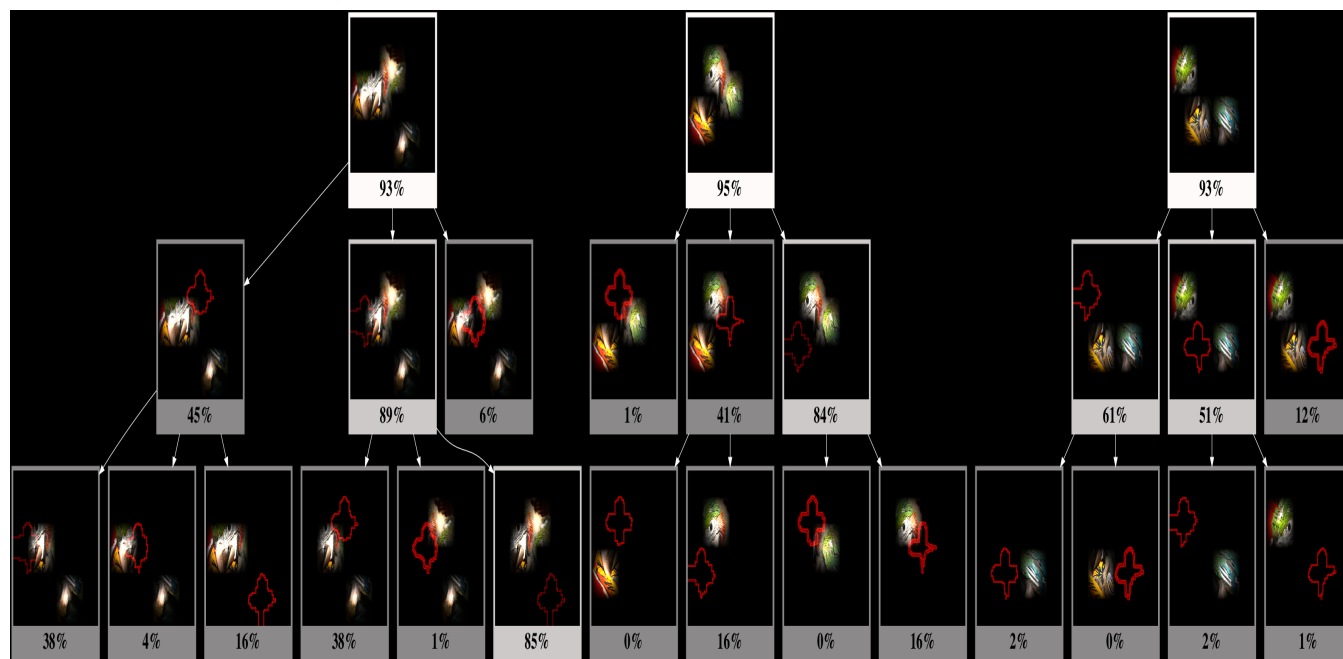
(a) Original Image



(b) Grad-CAM



(c) I-GOS



(d) SAG

7.7 Class: *Racecar*



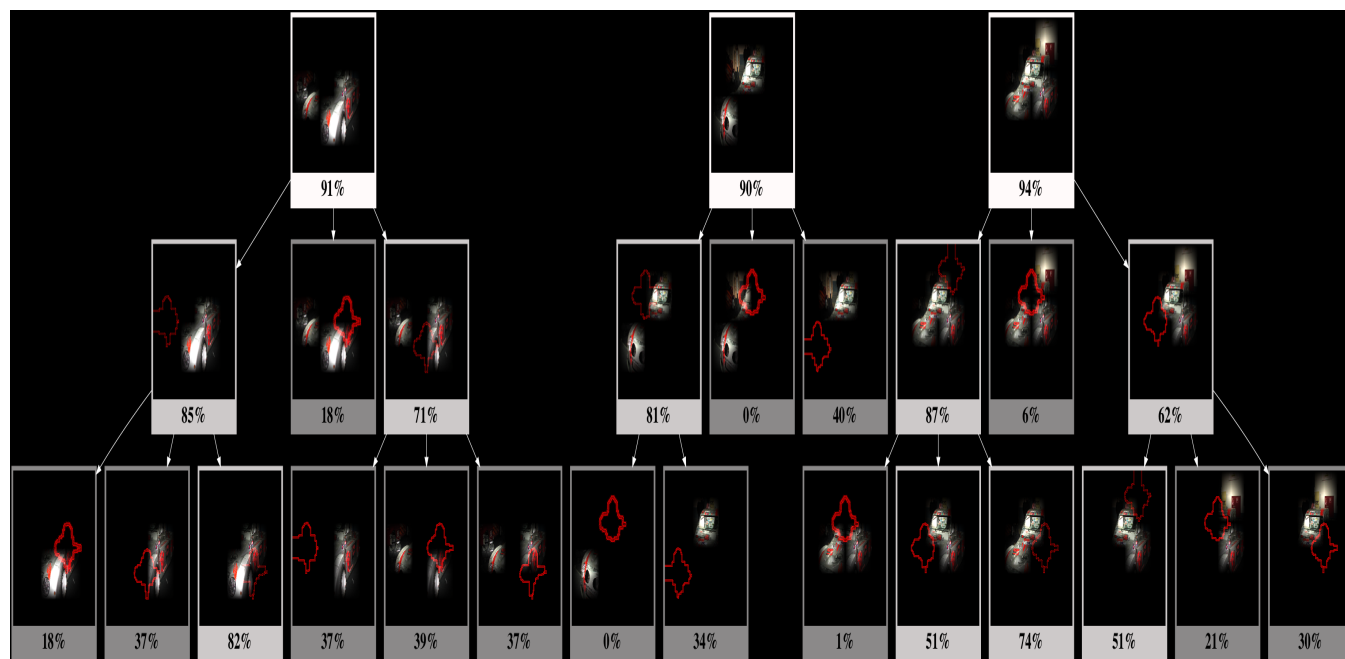
(a) Original Image



(b) Grad-CAM

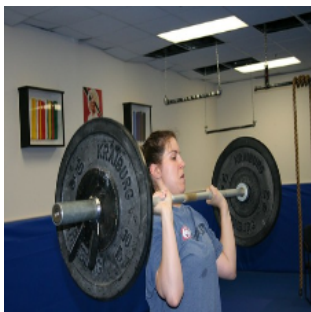


(c) I-GOS

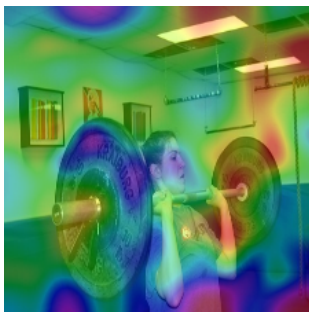


(d) SAG

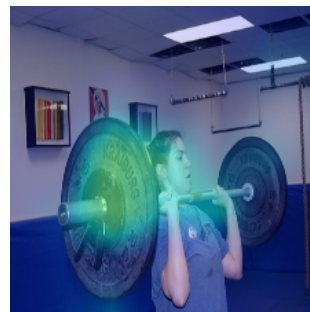
7.8 Class: *Barbell*



(a) Original Image



(b) Grad-CAM



(c) I-GOS

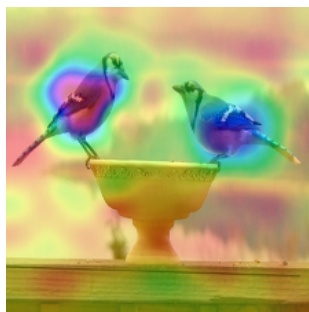


(d) SAG

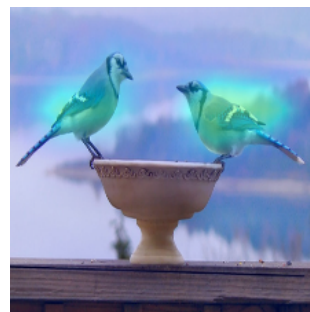
7.9 Class: *Jay*



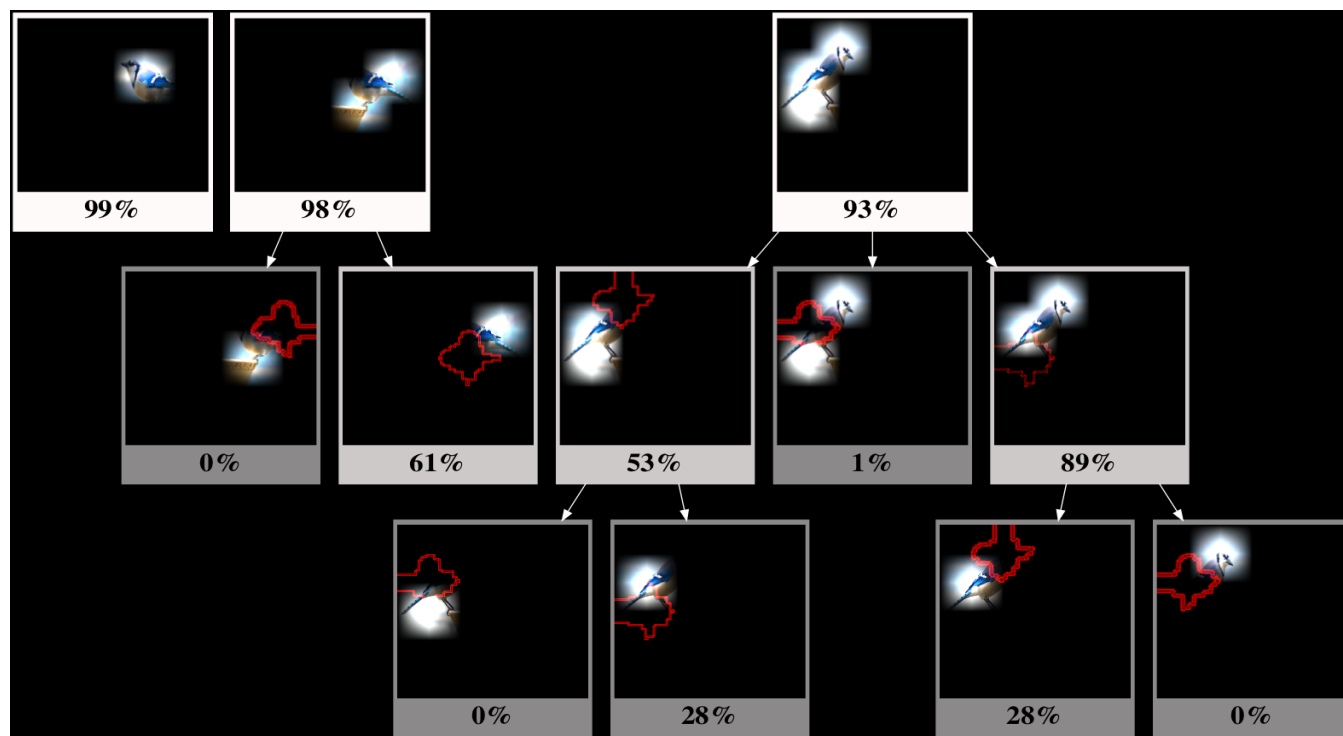
(a) Original Image



(b) Grad-CAM



(c) I-GOS

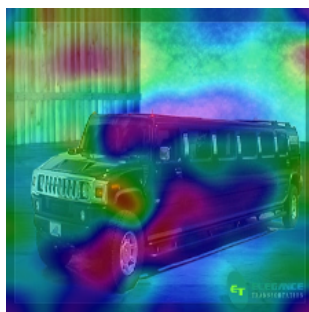


(d) SAG

7.10 Class: *Limousine*



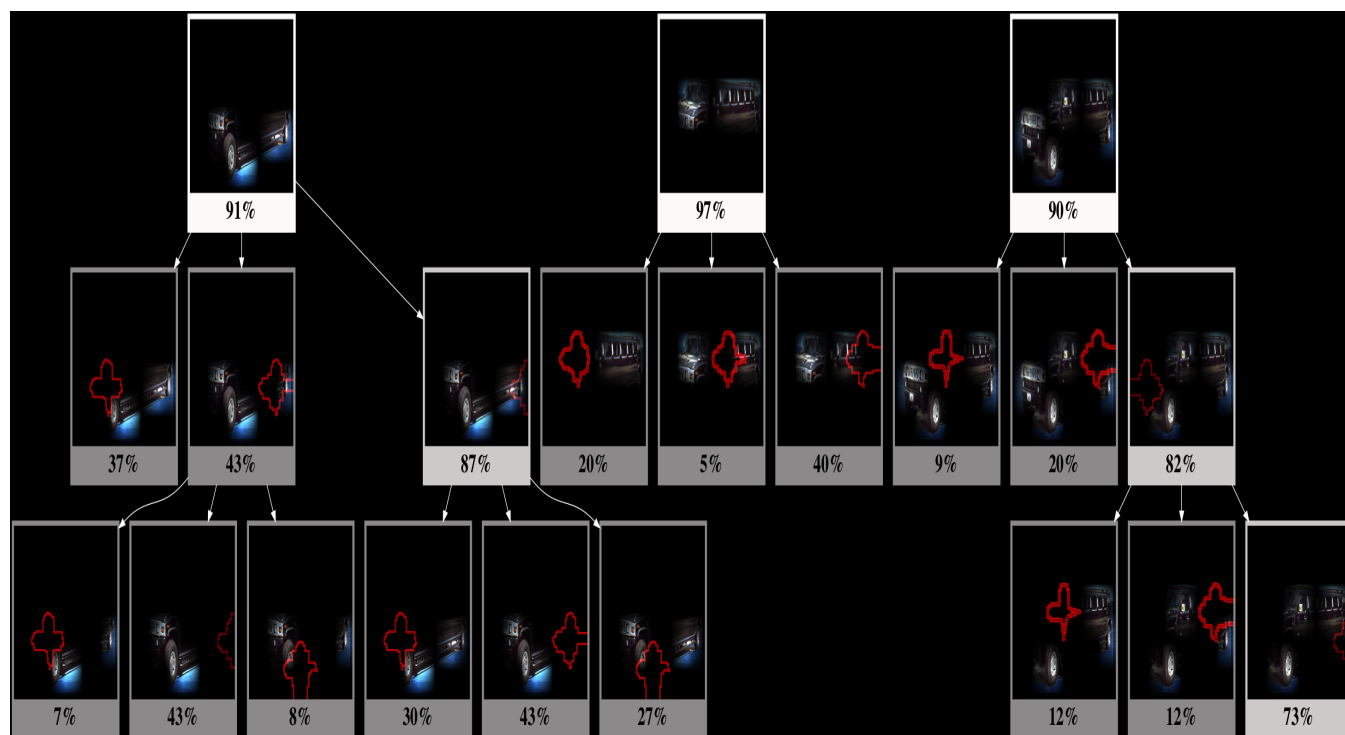
(a) Original Image



(b) Grad-CAM



(c) I-GOS



(d) SAG

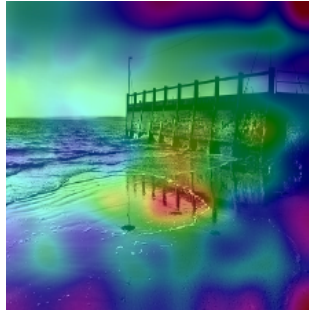
8 Appendix C - SAGs for debugging wrong predictions

Here we provide examples of SAGs for wrong predictions by VGG-Net. These SAG explanations provide interesting insights into the wrong decisions of the classifier. For contrast, we also show the corresponding Grad-CAM and I-GOS explanations for the wrong predictions.

8.1 Predicted class: *Shopping-cart*; True class: *Seashore*



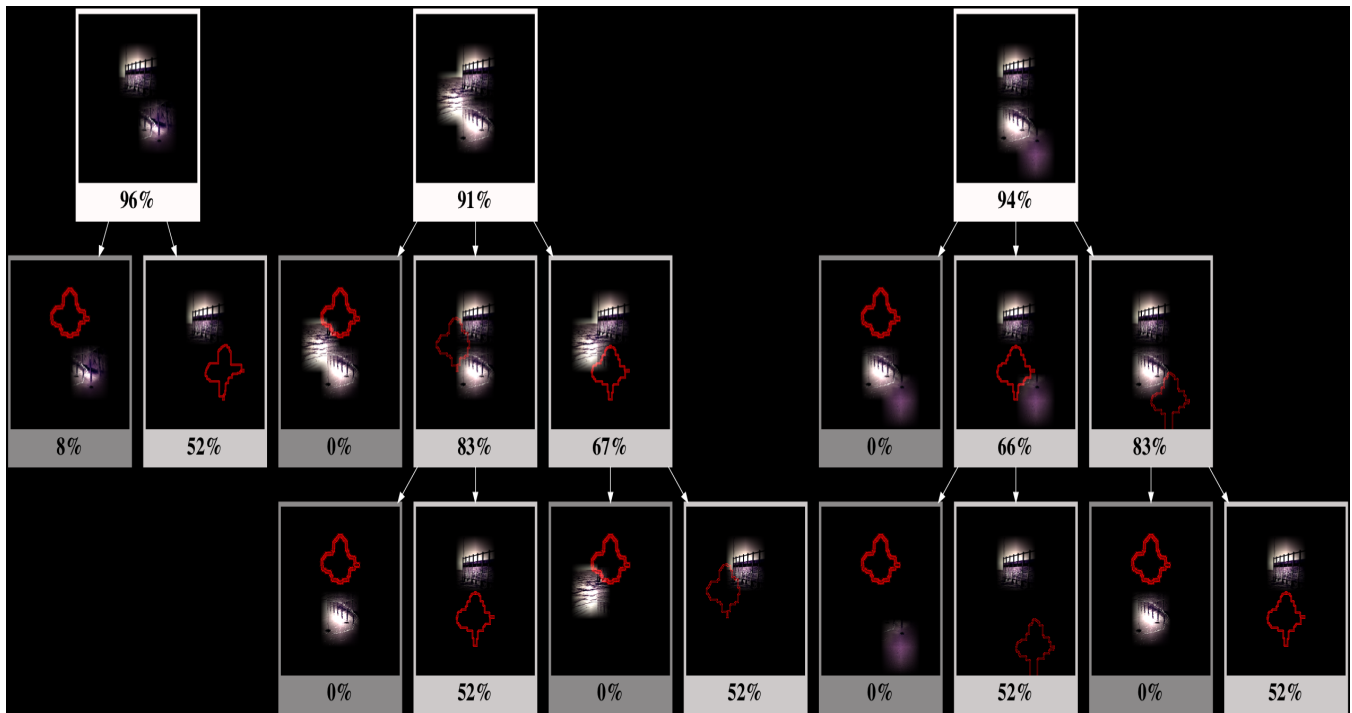
(a) Original Image



(b) Grad-CAM



(c) I-GOS



(d) SAG

8.2 Predicted class: *Pickup*; True class: *Limousine*



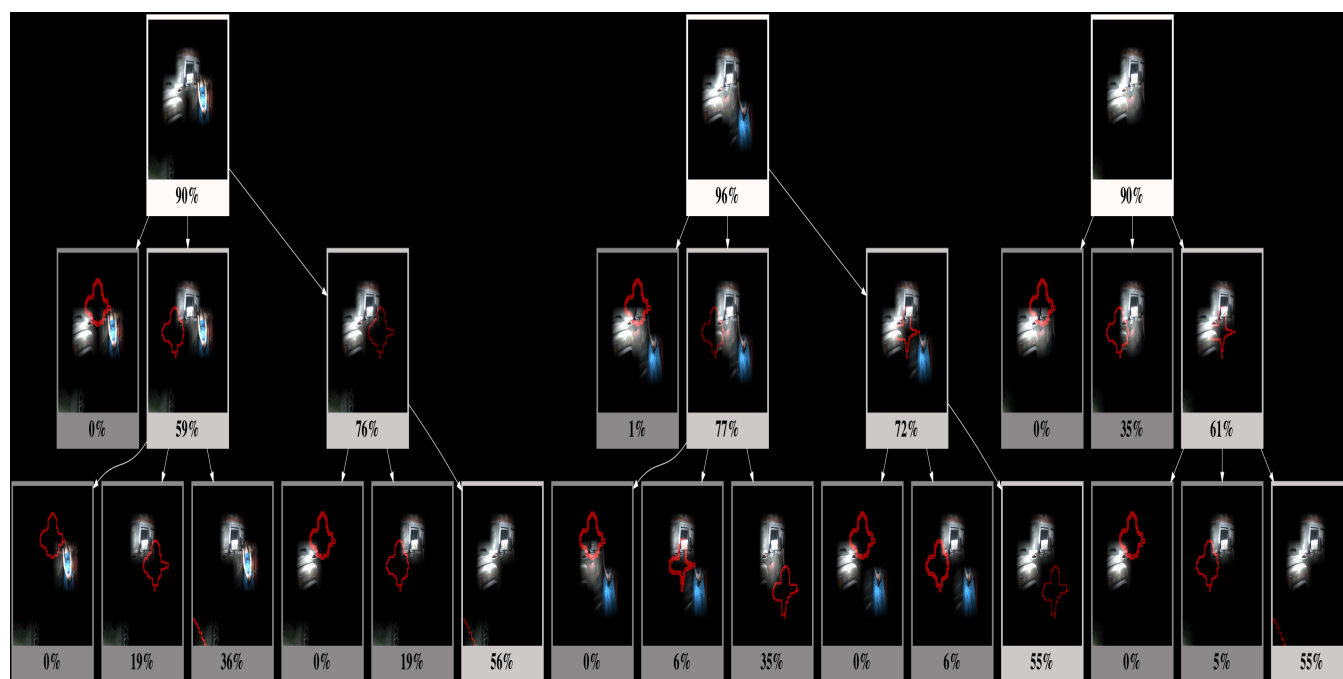
(a) Original Image



(b) Grad-CAM



(c) I-GOS



(d) SAG

8.3 Predicted class: *Golf-cart*; True class: *RV*



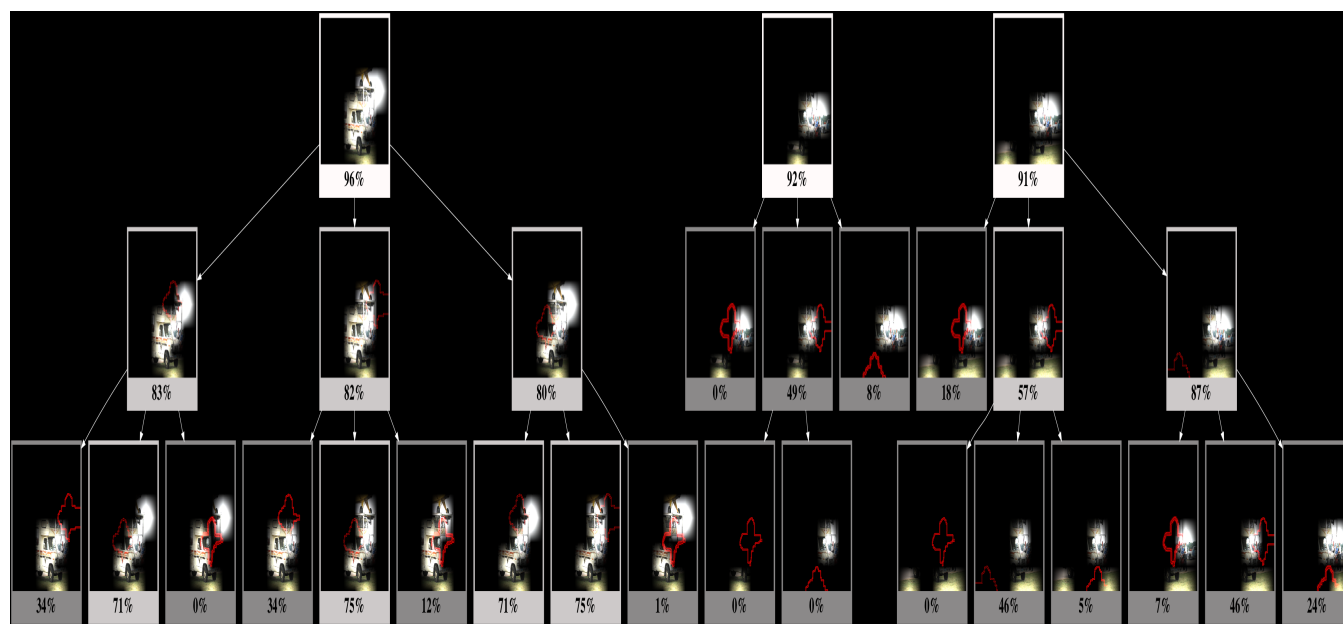
(a) Original Image



(b) Grad-CAM

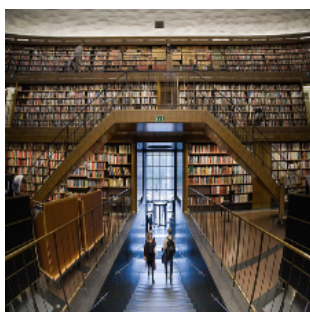


(c) I-GOS

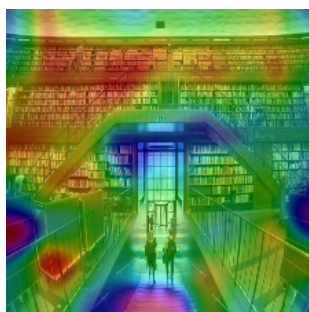


(d) SAG

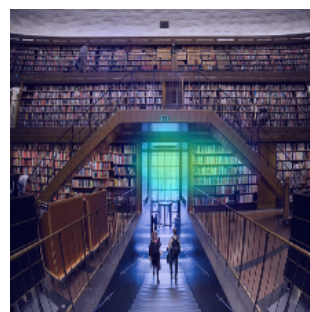
8.4 Predicted class: *Prison*; True class: *Library*



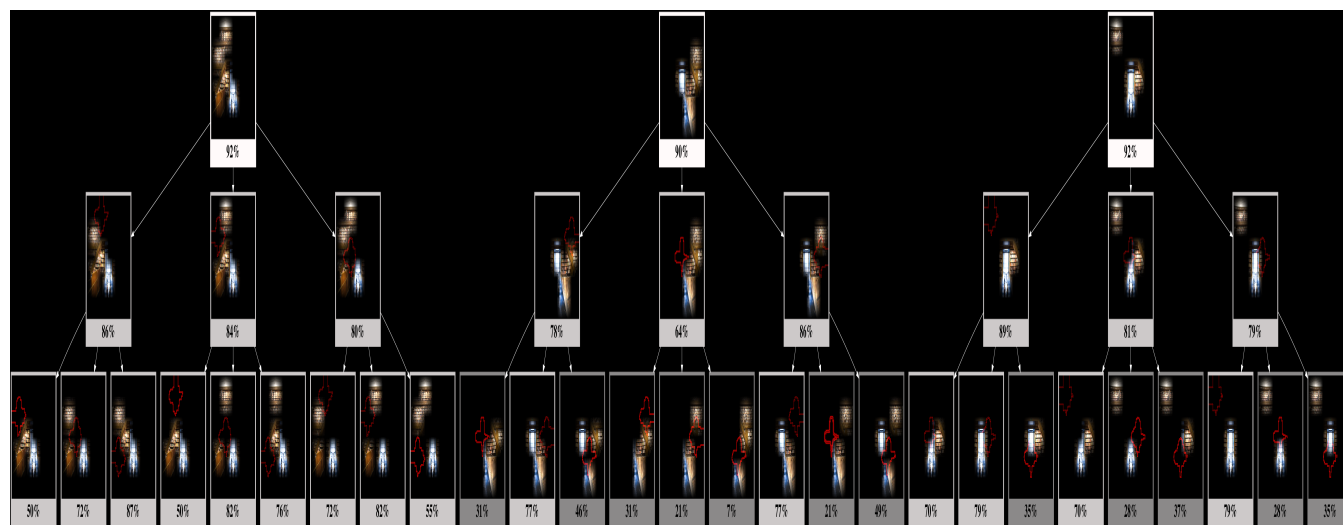
(a) Original Image



(b) Grad-CAM



(c) I-GOS

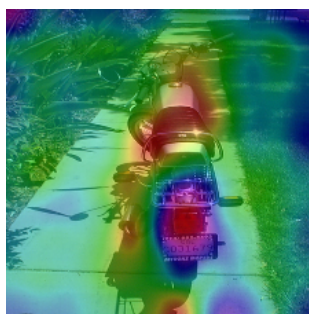


(d) SAG

8.5 Predicted class: *Shopping-cart*; True class: *Moped*



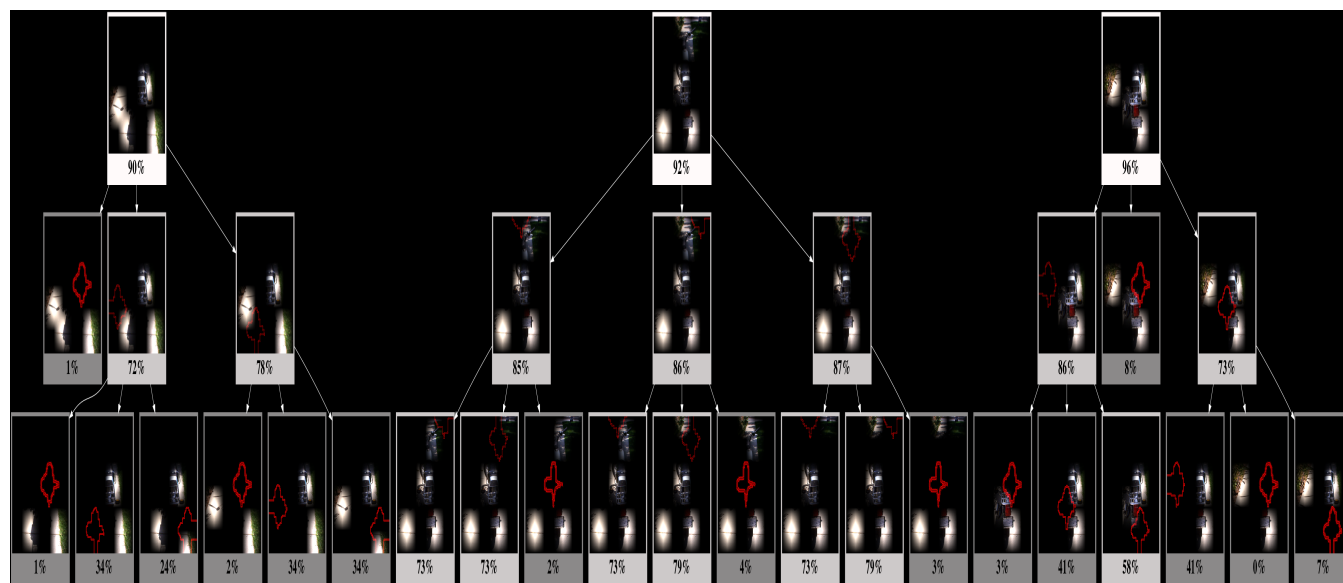
(a) Original Image



(b) Grad-CAM



(c) I-GOS



(d) SAG

8.6 Predicted class: *Space-shuttle*; True class: *Racecar*



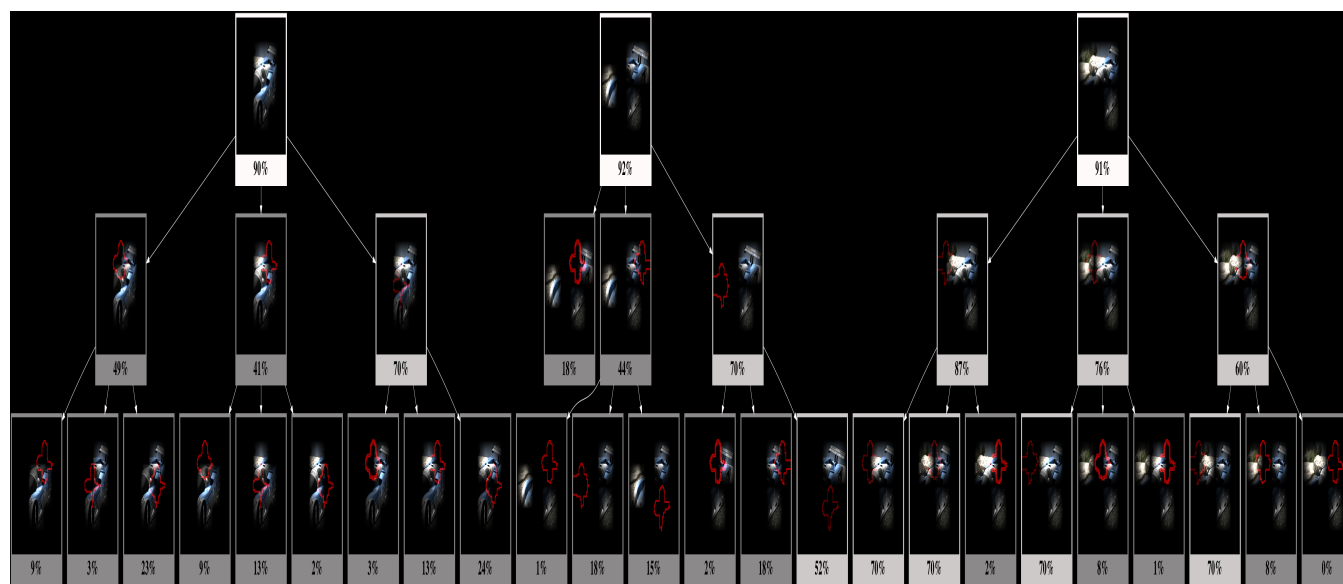
(a) Original Image



(b) Grad-CAM



(c) I-GOS



(d) SAG